J. Phys. B: At. Mol. Phys. 17 (1984) 4087–4101. Printed in Great Britain

Self-consistent core potentials for complex atoms: a semiclassical approach

Lorenzo J Curtis† and Richard R Silbar‡

† Department of Physics and Astronomy, University of Toledo, Toledo, Ohio 43606, USA
‡ Theoretical Division, Los Alamos National Laboratory, Los Alamos, New Mexico 87544, USA

Received 21 February 1984, in final form 26 June 1984

Abstract. A semiclassical self-consistent field method for specification of the structure of a complex atom is developed. The procedure utilises classical position probability densities and a modern version of the Bohr–Sommerfeld–Wilson quantisation condition. The semiclassical results are compared with non-relativistic quantum mechanical Hartree–Fock calculations, and energy eigenvalues and average values are found to be in remarkably close agreement. A relativistic extension of the semiclassical method is used to investigate the fine structure of highly ionised members of the Cu isoelectronic sequence. The calculations suggest two ways in which the observed break near $Z = 60$ in the screening parametrisation of this system could occur.

1. Introduction

Recent experimental advances have made possible the study of atomic systems that possess both high complexity and quasi-classical attributes. As one example, laser-produced and tokamak-produced plasmas and fast-ion-beam excitation methods provide access to the spectra of highly ionised heavy atoms (e.g., Reader and Luther 1981, Denne *et al* 1983, Johnson *et al* 1982), for which the many-electron problem becomes increasingly dominated by the high central charge of the nucleus. As another example, the development of laser and radio-frequency resonance techniques has made possible unprecedented precision in the measurement of highly excited Rydberg states (e.g., Cok and Lundeen 1981, Gallagher *et al* 1982).

However, modern theoretical quantum mechanical methods are difficult to apply when quantum numbers are high and the number of electrons is large. This has led to a resurgence of interest in semiclassical formulations (e.g., Percival and Richards 1975, Percival 1977, Berry and Mount 1972). Many of the difficulties inherent in the old Bohr–Sommerfeld–Wilson quantisation (Sommerfeld 1934) of periodic Kepler trajectories have been removed by the Einstein–Brillouin–Keller (Einstein 1917, Brillouin 1926, Keller 1958) reformulation and by the Maslov topological index (Maslov 1972). Semiclassical formulations with accuracies comparable with or exceeding those of quantum mechanical calculations have been made using, e.g., variational (Leopold and Percival 1980), perturbative (Leopold *et al* 1980), quantum defect (Jaffé and Reinhardt 1977) and core polarisation (Curtis 1981a) methods. The quantum

0022-3700/84/204087+15$02.25

mechanical formulation of complex many-electron atoms is usually described using some variant of the Hartree method (Hartree 1928, 1929), which iteratively forms a self-consistent central charge distribution by the superposition of single-electron position probability densities. We present here the formulation of a semiclassical analogue of the Hartree approach and applications to the sodium and copper isoelectronic sequences.

Although presently available *ab initio* methods are sufficiently accurate for many purposes, the classification of high-resolution atomic spectra makes very stringent demands. These considerations are especially troublesome for very heavy, very highly ionised, and very highly excited atomic systems. In these strongly relativistic regimes, compromises must be made in theoretical calculations, balancing the complications of a full relativistic treatment against the need to include non-central effects (Layzer and Bahcall 1962). This is particularly relevant to calculations of quantities that are sensitive to the inner part of the wavefunction. For example, theoretical methods that provide reliable predictions for gross energies and oscillator strengths, which derive their largest contributions from the outer parts of the wavefunctions, are often much less accurate in predicting fine-structure separations. Specialised theoretical approaches can improve the accuracy of fine-structure calculations, but this is often at the expense of a valid overall physical representation. Luc-Koenig (1980) and Detrich and Weiss (1982) have discussed the relationship between relativistic and non-relativistic descriptions of alkali-like fine structure and have concluded that a single-configuration relativistic calculation is equivalent to a multiconfiguration non-relativistic treatment that includes core polarisation. Both approaches are capable of predicting approximate trends in fine-structure separations on a 1% level of accuracy, but both also exhibit systematic discrepancies at higher levels of accuracy. In addition, Huang *et al* (1982) have recently pointed out that the relativistic Dirac–Hartree–Fock method produces spurious contributions from the gross structure that spill over into the fine structure unless special precautions are taken to ensure that configuration interaction and fractional parentage mixtures are forced to converge to the correct non-relativistic limit.

Motivated by the hope that semiclassical insights into many-electron core charge distributions might permit improvements in quantum mechanical calculations, we have formulated a semiclassical analogue of the Hartree self-consistent field calculation, and sought to determine how far this simple approach can be extended before breaking down. Although electron spin–spin and spin–other-orbit interactions, electron correlations and exchange effects are difficult to include in a semiclassical model, relativistic mass effects can be exactly included in the self-consistent Hamilton–Jacobi formulation of the Kepler problem, and spin–orbit magnetic interactions can also be simply added by a perturbative procedure.

We first review the generalised Bohr–Sommerfeld–Wilson quantisation rules as applied to atomic systems and then consider the application to non-penetrating and interpenetrating orbits in complex atoms in the central field approximation, using both non-relativistic and relativistic formulations. We next compare the results of our non-relativistic self-consistent semiclassical calculations for ions in the sodium isoelectronic sequence with those of a quantum mechanical Hartree–Fock program. Finally we apply the semiclassical formalism to the understanding of experimental observations of the fine structure of the $4p\,^2P$ term in the copper isoelectronic sequence. Our semiclassical calculations suggest two possible reasons for the 'break' that occurs in the screening parametrisation of this system near $Z = 60$.

2. The semiclassical self-consistent field method

Unless otherwise stated, quantities in the development to follow will be expressed by 'Rydberg atomic units', in which energies are in units of the Rydberg constant Ryd, distances are in units of the Bohr radius a_0, and action is in units of the Planck constant $\hbar$ (in these units the speed of light $c = 2/\alpha$, where α is the fine-structure constant). This unit system can be achieved by setting $\hbar = 2m = ke^2/2 = 1$ in all SI equations, where m is the reduced mass of the system, e is the magnitude of the charge quantum and k is the electrostatic force constant. Although this system differs from the 'Hartree atomic units' system (obtained by setting $\hbar = m = ke^2 = 1$) used in many quantum mechanics textbooks, it is the one used by most experimental and some theoretical atomic spectroscopists. In either system, both the energy unit (Ryd and 2 Ryd) and the distance unit (a_0) contain the reduced mass correction, and are not universal constants.

2.1. Semiclassical quantisation of the Hamilton–Jacobi equation

According to the Einstein–Brillouin–Keller quantisation rule, a generalised momentum p_i, its canonically conjugate coordinate q_i, and the corresponding quantum number n_i are related through the action integral I_i

$$I_i = (2\pi)^{-1} \oint \mathrm{d}q_i\, p_i = n_i + \mu_i/4 \qquad (n_i = 0, 1, 2, \ldots) \tag{1}$$

where μ_i is the Maslov index, which is 2 for librations and 0 for rotations. For a central potential expressed in spherical polar coordinates there are two librations and one rotation

$$I_\phi = n_\phi \qquad I_\theta = n_\theta + \tfrac{1}{2} \qquad I_r = n_r + \tfrac{1}{2}. \tag{2}$$

The angular integrals are readily performed (Goldstein 1980, pp 472–84), and can be combined to correspond to familiar angular momentum quantities. The connexion with the standard quantum numbers n, l and m_l is

$$L_z = I_\phi = n_\phi \to m_l \tag{3}$$

$$L = I_\phi + I_\theta = n_\phi + n_\theta + \tfrac{1}{2} \to l + \tfrac{1}{2} \tag{4}$$

$$n = I_\phi + I_\theta + I_r = n_\phi + n_\theta + n_r + 1 \to n_r + l + 1. \tag{5}$$

The radial action integral becomes

$$n - l - \tfrac{1}{2} = (2\pi)^{-1} \oint \mathrm{d}r\, k(r) \tag{6}$$

where $k(r)$ is the radial momentum or wavevector (measured in units $\hbar/a_0$)

$$k(r) = [E - V(r) - (l + \tfrac{1}{2})^2/r^2]^{1/2}. \tag{7}$$

For a bound system, both the total energy E and the potential energy $V(r)$ are inherently negative quantities. The eigenvalue $L^2 = (l + \frac{1}{2})^2$ that occurs here exceeds the quantum mechanical result $l(l+1)$ by $\frac{1}{4}$. A similar substitution must be made when the semiclassical WKB approximation is used to describe scattering processes, and is known as the 'Langer modification' (Langer 1937). A general prescription for converting the

For this non-penetrating electron orbit, the integral in the denominator of equation (14) can be analytically performed to yield Kepler's third law. The charge density also corresponds to a position probability density, and average values of the various contributions to the energy can be computed. For example,

$$\langle r^q \rangle = \int \mathrm{d}r\, \sigma(r) r^q. \tag{15}$$

2.3. Self-consistent charge for interpenetrating orbits

If all of the electrons in an atom are to be considered in a self-consistent manner, then each electron is governed by a separate action integral

$$n_i - l_i - \tfrac{1}{2} = \pi^{-1} \int \mathrm{d}r_i [E_i - V_i(r_i) - (l_i + \tfrac{1}{2})^2 / r_i^2]^{1/2} \tag{16}$$

where the potential is given by

$$V_i(r_i) = -2Z/r_i + \sum_{j \neq i} 2 \int \mathrm{d}r_j\, \sigma_j(r_j) |\overrightarrow{r_k - r_i}|^{-1}. \tag{17}$$

The electron–electron portion of the interaction can be written as a central potential by an expansion on Legendre polynomials

$$|\overrightarrow{r_j - r_i}|^{-1} = \sum_{K=0} (r_<^K / r_>^{K+1}) P_K(\cos \theta_{ij}) \tag{18}$$

where $r_<$ and $r_>$ are the lesser and greater of r_j and r_i. If we retain only the lowest order in K, the potential can be approximated by

$$V_i(r_i) = -2Z/r_i + \sum_{j \neq i} 2 \int \mathrm{d}r_j\, \sigma_j(r_j)/r_>. \tag{19}$$

Writing out the integral explicitly, the potential assumes the form that would be obtained computing the potential due a spherically symmetric distribution of charge (cf Cowan 1981, pp 181–3)

$$V_i(r_i) = -2[Z - S_i(r_i)]/r_i + 2w_i(r_i). \tag{20}$$

Here $S_i(r_i)$ is the charge enclosed by a Gaussian sphere of radius r_i

$$S_i(r_i) = \sum_{j \neq i} \int_0^{r_i} \mathrm{d}r\, \sigma_j(r) \tag{21}$$

and $w_i(r_i)$ is the contribution to the potential energy from the external charge

$$w_i(r_i) = \sum_{j \neq i} \int_{r_i}^{\infty} \mathrm{d}r\, \sigma_j(r)/r. \tag{22}$$

The neglect of higher-order contributions to the K sum is equivalent in the quantum mechanical problem to retaining only the lowest-order direct Slater integral $F0$. (The exchange Slater integrals are, of course, also absent in this classical formulation.) The value for $\sigma_i(r)$ can be obtained either from an initial estimate, or as a value deduced from a previous iteration of this process. The eigen-energy E_i can be determined from

the quantisation condition

$$n_i - l_i - \tfrac{1}{2} = \pi^{-1} \int \mathrm{d}r\, k_i(r) \tag{23}$$

for each i by numerical inversion.

Knowing E_i, the effective charge density can now be recomputed using

$$\sigma_j(r_j) = (k_j(r_j))^{-1} \left(\int \mathrm{d}r (k_j(r))^{-1} \right)^{-1}. \tag{24}$$

The results obtained from equation (24) can then be summed over j and compared with the assumed input value for each i. The entire process can then be iterated until convergence to a self-consistent set of values for E_i and $\sigma_j(r)$ is obtained.

From the self-consistent values for the charge distributions it is possible to compute, for each orbital, expectation values as in equation (15), and various contributions to the energy. The kinetic energy for the ith orbital is

$$\mathrm{KE}_i = \int_0^\infty \mathrm{d}r_i\, \sigma_i(r_i)[k_i^2(r_i) + (l_i + \tfrac{1}{2})^2 / r_i^2] \tag{25}$$

the electron–nucleus portion of the potential energy is

$$\mathrm{NPE}_i = -2Z \int_0^\infty \mathrm{d}r_i\, \sigma_i(r_i)/r_i \tag{26}$$

and the electron–electron portion is

$$\mathrm{EPE}_i(\mathrm{dir}) = \sum_{j \neq i} F0_{ij} \tag{27}$$

where $F0_{ij}$ is the direct Slater integral

$$F0_{ij} = 2 \int_0^\infty \mathrm{d}r_i\, \sigma_i(r_i) \int_0^\infty \mathrm{d}r_j\, \sigma_j(r_j)/r_>. \tag{28}$$

As in the quantum mechanical problem, the energy of the system is given by Koopmans' theorem (Koopmans 1934). The eigen-energy obtained in the inversion of equation (16) is related to the quantities above by

$$E_i = \mathrm{KE}_i + \mathrm{NPE}_i + \mathrm{EPE}_i \tag{29}$$

whereas, because of the double counting inherent in the paired electron–electron interactions, the total energy E of all of the electrons is given by

$$E = \sum_i (\mathrm{KE}_i + \mathrm{NPE}_i + \tfrac{1}{2}\mathrm{EPE}_i) = \sum_i (E_i - \tfrac{1}{2}\mathrm{EPE}_i). \tag{30}$$

In practice, the sum is more conveniently performed over n and l substates weighted by the occupation numbers, rather than over the individual electrons.

In analogy with the Hartree method, it is the total energy of the atom that has been determined jointly with the position probability density, and this quantity can be directly compared with experiment. It is possible to make an exact (non-perturbative) self-consistent relativistic extension of the method without increasing the complexity of the mathematics. A similar quantum mechanical formulation has been made by Cowan and Griffin (1976).

2.4. Relativistic formulation

Inclusion of relativistic mass effects requires only minor modifications of the equations already presented. The relativistic Hamiltonian formulation for a system bound by an electrostatic force derivable as the gradient of an attractive potential $V(r)$ is (in SI units)

$$E + mc^2 = [(pc)^2 + (mc^2)^2]^{1/2} + V(r). \tag{31}$$

E and $V(r)$ are again inherently negative, and if there are no magnetic vector potentials, p is the magnitude of the canonical vector momentum. Converting to Rydberg atomic units and solving for p^2 this becomes

$$p^2 = (E - V(r)) + \tfrac{1}{4}(E - V(r))^2\alpha^2. \tag{32}$$

In spherical polar coordinates, using the azimuthal quantisation and the Rydberg units, the generalised momenta become

$$p^2 = k^2(r) + (l + \tfrac{1}{2})^2/r^2. \tag{33}$$

Combining equations (32) and (33), the radial momentum is given by

$$k(r) = [E - V(r) - (l + \tfrac{1}{2})^2/r^2 + \tfrac{1}{4}(E - V(r))^2\alpha^2]^{1/2}. \tag{34}$$

Notice that this is an exact description of the relativistic electrostatic problem. Although spin magnetic effects are not automatically contained in the classical formulation, no truncations of relativistic expansions were made in obtaining equation (34). The quantisation integral can now be performed by substituting equation (34) into equation (23), but computation of the position probability density requires that the relation between radial speed and radial momentum of equation (13) be replaced by its relativistic counterpart (in SI units)

$$\mathrm{d}r/\mathrm{d}t = pc/[(pc)^2 + (mc^2)^2]^{1/2}. \tag{35}$$

Using the radial component of equation (35), expressed in Rydberg units, equation (12) becomes

$$\sigma(r)\,\mathrm{d}r = \frac{[1 + \alpha^2k^2(r) + \alpha^2(l + \tfrac{1}{2})^2/r^2]^{1/2}}{Tk(r)}\,\mathrm{d}r \tag{36}$$

with the normalising period T evaluated by integration as in equation (14).

For a non-penetrating orbit without polarisation $V(r) \to -2\zeta/r$, and the quantity under the square root in equation (34) is quadratic both with and without the α^2 correction, and the action integral can be performed exactly (cf Sommerfeld 1934, ch 5). For an interpenetrating but purely electrostatic system, $V(r)$ is as given in equation (17). Equation (34) can again be indexed with i as in equation (16), and the entire analysis repeated with no other changes. There is one subtlety here—the coefficient of r^{-2} in equation (34) becomes $(l + \frac{1}{2})^2 - (\alpha\zeta)^2$ relativistically (cf Sommerfeld 1934, p 255). For S states this leads to a sign change at $\zeta = 1/2\alpha = 68.5$ which causes a collapse to zero of the non-zero perihelion introduced into these states by the Langer modification. (A quantum mechanical analogue of this has been considered by Garcia (1984).)

2.5. Inclusion of the spin–orbit interaction

The previous section dealt only with the inertial portion of the relativistic problem, and neglected the magnetic interaction. These two contributions are inseparable in

the relativistic Dirac formulation of quantum mechanics, but in our semiclassical approach the effects must be individually accounted for, similar to Pauli relativistic corrections to the Schrödinger equation. However, there are difficulties in the covariant formulation of Hamiltonian mechanics when magnetic vector potentials are included (Goldstein 1980, pp 356–62), and there are ambiguities in the gauge definitions (cf, e.g., Mandel 1979). Thus, rather than attempting to include spin–orbit coupling in the self-consistent formulation of the quantised action integral, we have computed it perturbatively using the charge distribution determined as described in § 2.4. The interelectron spin–spin and spin–other-orbit interactions are non-central, and have been neglected so far in our calculation. For a spin $\frac{1}{2}$ term, the fine-structure splitting is given perturbatively to be (cf Cowan 1981, p 85)

$$\Delta V_i(\mathrm{so}) = (l+\tfrac{1}{2})\alpha^2 \int_0^\infty \mathrm{d}r\, \sigma_i(r)(Z - S_i(r))r^{-3} \tag{37}$$

where $S_i(r)$ is as defined in equation (21). For the non-penetrating case $\Delta V_i(\mathrm{so})$ is given by the Sommerfeld expansion (Curtis 1977) with an effective charge $Z - N + 1$.

3. Numerical methods

A computer code has been written to perform the calculations described in § 2. Initial charge distributions were obtained from the nodeless analytic approximate wavefunctions of Slater (1930). We then successively iterated until self-consistency was achieved. Charge distributions obtained from one element in an isoelectronic sequence could then serve as the starting values for another element of differing nuclear charge. Integrations were performed using the trapezoidal approximation, with an exponentially incremented radial mesh. The mesh began at one tenth the distance to the non-relativistic 1s perihelion for the bare nuclear charge, and extended to 1.2 times the distance to the non-relativistic 4p aphelion for the fully screened nuclear charge. The number of mesh points was varied between 128 and 512 to test the accuracy of the trapezoidal approximation, and no significant differences occurred. The action integral of equation (16) was inverted by the Newton–Raphson method to yield the eigenvalue E_i for a given n_i and l_i. The normalisation integral of equation (24) could be performed by the trapezoidal method for all regions except at the turning points, where poles occur. The integrals within the endpoint mesh panels were therefore performed analytically, using a numerically differentiated Taylor expansion about the endpoint. The iterative convergence to a self-consistent charge distribution was tested by computing the sum of the squares of the relative changes of the total charge in each panel with each succeeding iteration. For the lower stages of ionisation in a sequence, convergence sometimes did not occur. For the cases discussed in this paper convergence was achieved tc within 0.1% in four iterations or less.

4. Applications

The computer code developed for this semiclassical formulation was initially tested through non-relativistic calculations for several ions in the sodium isoelectronic sequence, and compared with quantum mechanical Hartree–Fock calculations for the

same ions. The code was then applied to the study of certain features in the fine structure of ions in the copper isoelectronic sequence. The phenomenological interpretability and the ease with which relativistic effects are incorporated in the semiclassical approach provide insights into these features.

4.1. Ground configuration energies for the sodium isoelectronic sequence

Non-relativistic calculations for the $1s^2 2s^2 2p^6 3s$ ground configuration for the sodium-like P^{4+}, Fe^{15+} and Mo^{33+} ions were made using both the semiclassical self-consistent field program (SCSCF) described above and the quantum mechanical non-relativistic Hartree–Fock program (NRHF) developed by Froese Fischer (1978). A summary of the results, classified according to the contributions of the kinetic energy, the nucleus–electron potential energy and the electron–electron direct and (for the quantum mechanical case) exchange potential energies for each subshell, is given in table 1. For the quantum mechanical case, the electron–electron energies were deduced from the Slater integrals $F0$ and $F2$ for the direct interaction, and from $G0$ and $G1$ for the exchange interaction (cf Cowan 1981, p 163). For the semiclassical case, the only electron–electron energy included is $F0$, as defined in equation (28).

Despite the apparent simplicity of the semiclassical model, there is close agreement between the SCSCF and NRHF methods that improves with increasing stage of ionisation.

Table 1. Comparison of a quantum mechanical Hartree–Fock calculation with the SCSCF method for the Na isoelectronic sequence.

	P^{4+}		Fe^{15+}		Mo^{31+}	
	QM	Class.	QM	Class.	QM	Class.
1s KE	212.48	213.22	651.98	645.57	1723.10	1720.32
NPE	−437.26	−437.47	−1327.70	−1317.38	−3486.80	−3482.38
EPE(dir)	61.70	61.44	119.24	116.62	202.60	205.46
EPE(exc)	−1.17	—	−2.79	—	−5.21	—
2s KE	31.93	27.57	123.81	94.22	365.67	349.70
NPE	−85.20	−79.51	−289.75	−255.15	−803.58	−786.07
EPE(dir)	36.75	35.93	72.73	68.22	124.87	124.50
EPE(exc)	−2.63	—	−5.18	—	−8.84	—
2p KE	29.80	27.52	120.71	109.57	361.00	356.48
NPE	−81.55	−78.78	−285.38	−272.78	−797.75	−792.79
EPE(dir)[a]	38.51	38.51	78.62	77.37	133.92	137.52
EPE(dir)[b]	−0.71	—	−1.49	—	−2.61	—
EPE(exc)	−0.99	—	−2.05	—	−3.59	—
3s KE	5.83	5.72	39.15	34.25	135.74	134.52
NPE	−25.12	−24.44	−109.24	−102.27	−326.94	−325.07
EPE(dir)	14.80	14.32	35.20	33.25	63.90	63.62
EPE(exc)	−0.25	—	−0.77	—	−1.51	—
Subtotal[c]	−664.46	−658.61	−2296.00	−2279.20	−6445.90	−6430.97
Total	−673.47	—	−2315.00	—	−6479.30	—

[a] QM portion arising from sum over $F0$ of equation (27).
[b] QM portion arising from $F2$.
[c] Total exclusive of $F2$ and $G1$ contributions.

(With either method the central field assumption improves with higher nuclear charge.) For this simple alkali-like system, the neglect of exchange and higher-order direct electron–electron interactions in the SCSCF approach introduces only small discrepancies. The SCSCF calculations exhibit a slight tendency to be smaller in magnitude than the NRHF values. The largest disagreements occur for the 2s orbital, but it is well known that the 2s wavefunction has an even poorer correspondence with the classical limit than the 1s. The 2s is the only S state which has exactly two antinodes in its quantum mechanical position probability density, and the inner antinode behaves like the perihelion of a classical state of angular momentum higher than S. Notice that without the Langer modification S states would have no perihelion, and the quantum mechanical 2s and 2p states would exchange their classical roles. Correspondingly, if the Langer modification is omitted from the SCSCF calculation, the 2p becomes more tightly bound than the 2s.

Figure 1 displays a plot of the SCSCF and NRHF calculations for the radial charge distribution of the neon-like core as seen by the 3s electron in an Fe^{15+} ion. The classical distribution is much more sharply peaked due to the poles at the perihelions and aphelions of the individual orbits that are summed in this plot. It is clear that the quantum numbers of these states are too small to expect the quantum mechanical distribution to approach the correspondence limit. Nevertheless, as can be seen from table 1, the expectation values obtained from the two distributions are very nearly the same. Thus the correspondence limit is reached much more easily for expectation values than for wavefunctions.

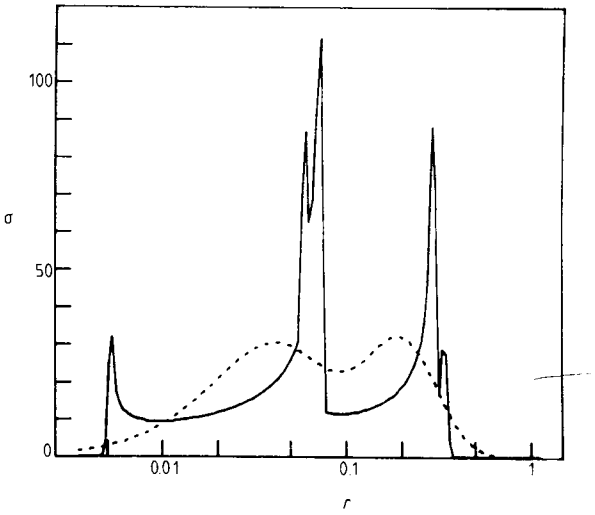

Figure 1. Position probability for the $1s^2 2s^2 2p^6$ core of the sodium-like Fe^{15+} ion, as seen by the 3s ground-state orbital plotted against orbital radius. The full curve represents the semiclassical SCSCF calculation, the broken curve represents the quantum mechanical NRHF calculation.

4.2. Regularities in the observed fine structure of the 4p ^2P term in the Cu isoelectronic sequence

One of the primary reasons for undertaking this semiempirical study was to gain insights into the phenomenological origin of isoelectronic linearities observed when

fine-structure separations of highly ionised atoms are formulated using the extended regular doublet law.

Since *ab initio* quantum mechanical calculations cannot presently provide the high accuracies often needed for spectroscopic classification, semiempirical extrapolation methods have been developed which possess the requisite precision. The extended regular doublet law (Edlén 1964) is one such method. It achieves a reparametrisation by replacing the nuclear charge Z by an effective screened charge Z_S in the best available analytic expression for the fine structure in a corresponding hydrogen-like atom. The extracted quantity Z_S has a slow and regular isoelectronic variation and provides a reliable and generally applicable means of predicting fine structure separations whenever a substantial body of experimental data is already available. In addition, this exposition of the data reveals regularities not predicted by theoretical calculations.

The nature of these regularities is illustrated in figure 2. The observed fine-structure separations (Reader and Luther 1981, Reader 1983 and earlier references cited by Curtis 1981b) of the $4p\ ^2P$ terms in the Cu isoelectronic are here displayed in a plot of the effective screening parameter against the reciprocal effective screened change as defined by the extended regular doublet law. The full straight line denotes a fit to the data with $32 < Z < 60$. No theoretical explanation for this linearity has yet been offered, but the same linear behaviour has been observed in many other isoelectronic sequences (e.g. Edlén 1964, Curtis and Ramanujam 1983a, b). For $Z > 60$ this linearity appears to break down, but in an interesting manner. Figure 3 is an enlargment of the region near $Z = 60$, and shows a break in the slope at that point. The full line denotes the fit to the data with $Z < 60$, whereas the broken line denotes a similar fit to the data with $Z > 60$. These two straight-line fits describe the entire isoelectronic body of data to within 1 part in 10^4. If a similar plot of the $4d\ ^2D$ fine-structure separations is made, the linearity persists over the entire range of data, with *no* break in the slope.

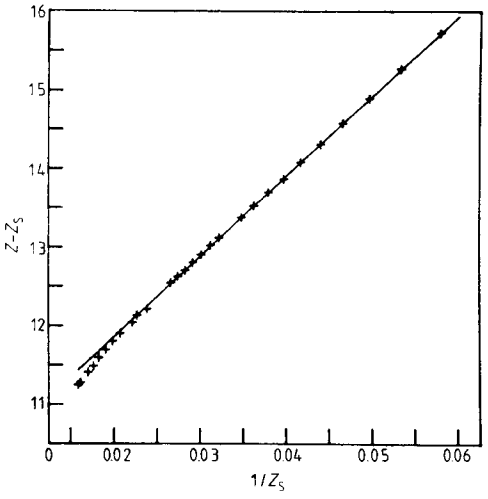

Figure 2. Plot of the effective screening parameter against the reciprocal effective screened charge for the $4p\ ^2P$ observed fine structure of the Cu isoelectronic sequence. The line denotes an empirical straight-line fit to the data with $Z < 60$.

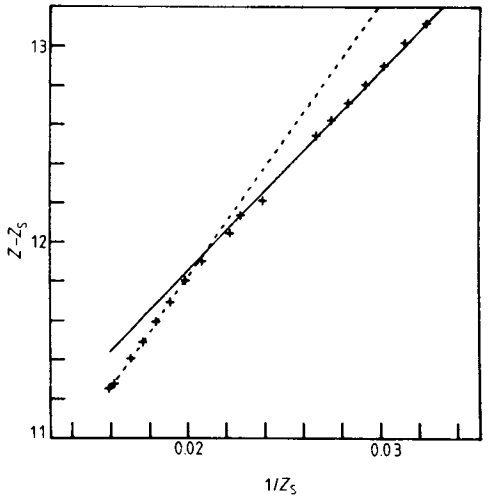

Figure 3. Enlarged view of figure 2 in the region of $Z = 60$. The dotted line is an empirical straight-line fit to the data with $Z > 60$.

Although the origin of this empirical linearity is unclear, the discontinuity in slope is suggestive of some kind of restructuring in the atomic configuration, which might have a classical explanation. These results illustrate the continuing validity of the statement of Layzer (1959) that the current theory of complex atomic spectra 'predicts simple regularities in the structure of term spectra that are not observed, and it does not predict the observed regularities, which are as simple as, but qualitatively different from, the predicted ones'.

For the Cu isoelectronic sequence Dirac–Hartree–Fock calculations (Cheng and Kim 1978) provide predictions for low-lying ^{2}P and ^{2}D levels that are accurate at the level of a few per cent. These calculations underestimate the splittings by 7% at $Z = 32$, and the underestimate reduces to 0.25% for $Z > 60$. However, when these calculations are plotted as screening parameters as in figure 2, there is a gentle downward curvature throughout, with neither the linear region nor the break in slope shown in figures 2 and 3. We have also used wavefunctions obtained from a standard Dirac–Hartree–Fock program (Desclaux 1975) to examine the inner portions of the position probability densities in the sequence for sudden isoelectronic shifts, but no such shifts were found. Thus the discontinuity may arise from mechanisms not included in these relativistic codes. Since the empirical linearity also exists for multiple-valence-electron systems (cf Curtis and Ramanujam 1983a, b) where theoretical predictions are much less accurate, we have sought a qualitative understanding by this semiclassical method.

Calculations were made for the $1s^22s^22p^63s^23p^63d^{10}4p$ configuration for ions from Kr^{7+} to U^{63+}, using both the relativistic and the non-relativistic options in the SCSCF program. Here again the non-relativistic results were compared with parallel calculations using the NRHF program. Despite the increased complexity of the system, agreement between the SCSCF and NRHF calculations was very similar to that shown in table 1 for the Na sequence. Comparisons were then made between the non-relativistic and relativistic SCSCF calculation, and semiclassical interpretations were sought for the fine-structure features described above. Isoelectronic comparisons were made, for example, of the distributions of the charges, the relative positions of the perihelions

and aphelions of the individual orbitals and the perturbatively computed spin–orbit energy.

The positions of the perihelions and aphelions for each of the seven orbitals for $Z = 42$, 62 and 82 are presented in table 2. There are several trends that should be noted: (i) the S-state perihelions are pulled in increasingly sharply with n in the relativistic calculation; (ii) the S-state perihelions collapse into the nucleus for $Z > 68$; and (iii) in the relativistic calculation the 1s aphelion shrinks inside the perihelions of the entire np Rydberg series near $Z = 60$. We shall discuss each of these trends separately.

Table 2. Classical perihelion and aphelion distances computed by the SCSCF method for the Cu isoelectronic sequence.

	Perihelion			Aphelion		
Configuration	$Z = 42$	$Z = 54$	$Z = 74$	$Z = 42$	$Z = 54$	$Z = 74$
Non-relativistic						
1s	0.0032	0.0025	0.0018	0.045	0.035	0.025
2s	0.0030	0.0024	0.0017	0.208	0.157	0.113
2p	0.0346	0.0263	0.0191	0.179	0.134	0.096
3s	0.0030	0.0023	0.0017	0.564	0.410	0.283
3p	0.0317	0.0240	0.0172	0.560	0.399	0.272
3d	0.1268	0.0903	0.0626	0.509	0.350	0.234
4p	0.0313	0.0236	0.0169	1.386	0.880	0.555
Relativistic						
1s	0.0021	0.0009	0	0.039	0.026	0.013
2s	0.0019	0.0003	0	0.188	0.130	0.078
2p	0.0336	0.0253	0.0172	0.176	0.132	0.092
3s	0.0019	0.0002	0	0.520	0.353	0.215
3p	0.0307	0.0229	0.0154	0.557	0.398	0.261
3d	0.1259	0.0908	0.0613	0.512	0.356	0.232
4p	0.0304	0.0225	0.0150	1.389	0.874	0.539

(i) Classically, the orbital speed is inversely proportional to the radial distance. Since S states are the most penetrating and rapidly moving orbitals they exhibit the largest relativistic shifts. (The attractive nature of the relativistic shift can be made plausible by considering time dilation in the highly attractive inner region.) For a given Rydberg series the non-relativistic perihelion distances tend to decrease slightly with increasing n. The speed and relativistic shift increase with n, enhancing this tendency sharply.

(ii) As discussed in § 2.4, the small but finite perihelion of the S states introduced by the Langer modification collapses relativistically for $Z - S_i > 68.5$. The approach to this collapse causes difficulties in both the calculation of the integration mesh and in the physical description of the passage through the nucleus. (The finite size of the nucleus has been neglected in the present simple stage of development of the semiclassical model.)

(iii) As can be seen from table 2, the aphelion of the 1s orbital is outside the perihelions of the p Rydberg series for $Z = 42$, but is drawn inside them by $Z = 74$.

The crossing occurs in the vicinity of $Z = 60$. This crossing is a purely relativistic effect which was described above, and the non-relativistic SCSCF calculation shows no such crossing. The exact position of the crossing is difficult to determine because the self-consistent convergence is disturbed by it, and results become very sensitive to the initial trial charge distribution. When the 1s aphelion is inside the p perihelions it screens them from the nuclear attraction, and they move even further out. When the 1s aphelion is outside the p perihelion it screens them less and they move even further in. Thus the classical crossing cannot occur in a smooth isoelectronic manner, but rather as a sudden and discontinuous jump from one configuration of charge to another. Although the primary effect of the shrinking of the 1s aphelion inside the np perihelions is an increase in the screening, many secondary effects could account for the observed decrease in screening (e.g. Rose *et al* 1978). Improved relativistic quantum mechanical calculations including e.g., electron correlations and exchange core polarisation (Holmgren *et al* 1976, Lee *et al* 1976) might elucidate these results.

Relativistic SCSCF calculations for the spin–orbit energy yielded an isoelectronic behaviour qualitatively similar to that seen in figures 2 and 3, a roughly linear slope of $Z - Z_S$ plotted against $1/Z_S$ that is steeper for higher Z. However, owing to the instabilities introduced by the 1s–np crossing and the collapse of the S perihelions, the results were too sensitive to the initial charge distribution to permit quantitative comparison at this time. Non-relativistic SCSCF calculations of the spin–orbit energy were in close agreement with the results obtained by the quantum mechanical NRHF program, but these non-relativistic results have the wrong trend when displayed on the screening parameter plot (rather than decreasing, the screening parameter increases with increasing Z).

5. Conclusions

From this study we conclude that, while the semiclassical approach is no substitute for a quantum mechanical Hartree–Fock calculation, it does provide a reasonably accurate qualitative description of a complex atom. It contains much of the physical essence of the quantum mechanical formulation, with the advantages of an obvious classical interpretation and a simple means for the self-consistent inclusion of kinetic relativistic effects. The application of the semiclassical approach to the study of the observed break in the slope of the screening parametrisation of the fine structure of the 4p term in the Cu sequence revealed two classically discontinuous mechanisms in the appropriate region. Substantial improvements in quantum mechanical calculations will be necessary to achieve the experimental spectroscopic accuracies for these intervals. Semiclassical formulations such as this may provide insights into how such improvements could be achieved.

Acknowledgments

This work was supported by the US Department of Energy, through the Fundamental Interactions Branch, Division of Chemical Sciences, Office of Basic Energy Sciences, under contract number DE-AS-05-80ER10676, and the Division of Nuclear Physics, Office of High Energy and Nuclear Physics.

References

Berry M V and Mount K E 1972 *Rep. Prog. Phys.* **35** 315–97
Brillouin M L 1926 *J. Physique* **7** 353–68
Cheng K-T and Kim Y-K 1978 *At. Data Nucl. Data Tables* **22** 547–63
Cok D R and Lundeen S R 1981 *Phys. Rev.* A **23** 2488–95
Cowan R D 1981 *The Theory of Atomic Structure and Spectra* (Berkeley: University of California Press)
Cowan R D and Griffin D C 1976 *J. Opt. Soc. Am.* **66** 1010–4
Curtis L J 1977 *J. Phys. B: At. Mol. Phys.* **10** L641–5
—— 1981a *J. Phys. B: At. Mol. Phys.* **14** 1373–86
—— 1981b *J. Phys. B: At. Mol. Phys.* **14** 631–40
Curtis L J and Ramanujam P S 1983a *Phys. Scr.* **27** 417–21
—— 1983b *J. Opt. Soc. Am.* **73** 979–84
Denne B, Hinnov E, Suckewer S and Cohen S 1983 *Phys. Rev.* A **28** 206–8
Desclaux J P 1975 *Comput. Phys. Commun.* **9** 31–45
Detrich J and Weiss A W 1982 *Phys. Rev.* A **25** 1203–5
Edlén B 1964 *Handbuch der Physik* vol 27 (Berlin: Springer) pp 80–220
Einstein A 1917 *Verhand. Deut. Phys. Ges.* **19** 82–92
Froese Fischer C 1978 *Comput. Phys. Commun.* **14** 145–53
Gallagher T F, Kachru R and Tran N H 1982 *Phys. Rev.* A **26** 2611–22
Goldstein H 1980 *Classical Mechanics* 2nd edn (Cambridge, MA: Addison-Wesley)
Garcia J D 1984 *Bull. Am. Phys. Soc.* **29** 818
Hartree D R 1928 *Proc. Camb. Phil. Soc.* **24** 89–110, 111–32, 426–37
—— 1929 *Proc. Camb. Phil. Soc.* **25** 310–4
Holmgren L, Lindgren I, Morrison J and Mårtensson A-M 1976 *Z. Phys.* A **276** 179–85
Huang K-N, Kim Y-K, Cheng K-T and Desclaux J P 1982 *Phys. Rev. Lett.* **48** 1245–8
Jaffé C and Reinhardt W P 1977 *J. Chem. Phys.* **66** 1285–9
Johnson B M, Jones K W, Kruse T H, Curtis L J and Ellis D G 1982 *Nucl. Instrum. Meth.* **202** 53–8
Keller J B 1958 *Ann. Phys., NY* **4** 180–8
Koopmans T 1934 *Physica* **1** 104–13
Langer R E 1937 *Phys. Rev.* **51** 669–76
Layzer D 1959 *Ann. Phys., NY* **8** 271–96
Layzer D and Bahcall J 1962 *Ann. Phys., NY* **17** 177–204
Lee T, Rodgers J E, Das T P and Sternheimer R 1976 *Phys. Rev.* A **14** 51–5
Leopold J G and Percival I C 1980 *J. Phys. B: At. Mol. Phys.* **13** 1037–47
Leopold J G, Percival I C and Tworkowski A S 1980 *J. Phys. B: At. Mol. Phys.* **13** 1025–36
Luc-Koenig E 1980 *J. Physique* **41** 1273–84
Mandel L 1979 *Phys. Rev.* A **20** 1590–2
Maslov V P 1972 *Théorie des Perturbations et Méthods Asymptotiques* (Gauthier-Villars, Paris: Dunod)
Percival I C 1977 *Adv. Chem. Phys.* **36** 1–61
Percival I C and Richards D 1975 *Adv. At. Mol. Phys.* **11** 1–82
Reader J 1983 private communication
Reader J and Luther G 1981 *Phys. Scr.* **24** 732–7
Rose S J, Grant I P and Pyper N C 1978 *J. Phys. B: At. Mol. Phys.* **11** 1171–6
Slater J C 1930 *Phys. Rev.* **36** 57–64
Sommerfeld A 1934 *Atomic Structure and Spectral Lines* vol 1, 3rd edn (revised) (London: Methuen)